Chemical Engineering Journal 103 (2004) 59–67

Chemical Engineering Journal

www.elsevier.com/locate/cej

Propane oxidative dehydrogenation on Cs-doped Cr-Mo-Al-O catalyst: kinetics and mechanism

B.Y. Jibril[a,*], S.M. Al-Zahrani[a], A.E. Abasaeed[a], R. Hughes[b]

[a] *Chemical Engineering Department, King Saud University, P.O. Box 800, Riyadh 11421, Saudi Arabia*
[b] *Chemical Engineering Unit, University of Salford, Maxwell Building, The Crescent, Salford, Manchester M54WT, UK*

Received 2 December 2003; accepted 23 March 2004

Abstract

Previous kinetic study reports on oxidative dehydrogenation (OXD) have suggested different mechanisms—Mars-van Krevelen (MV), Langmuir–Hinshelwood (L–H) and Rideal—depending on the nature of the catalyst. Earlier, we have demonstrated that Cs-Cr-Mo-Al-O is active and selective as a catalyst in propane oxidative dehydrogenation (POD). Here results of the reaction kinetic study on the catalyst at 300–340 °C are reported. Propane is oxidatively dehydrogenated to propene. Carbon dioxide is also produced directly from propane. Further oxidation of propene produced mainly CO. Rates of propane consumption and propene production are not significantly affected by changes in oxygen partial pressure, indicating a Mars-van Krevelen reaction mechanism. On the other hand, rates of CO_2 and CO productions have shown strong dependence on the partial pressure. Thus, oxygen species of difference types may be involve in the two cases.

Keywords: Oxidative dehydrogenation; Propane; Propene; Kinetics; Mechanism

1. Introduction

Oxidative dehydrogenation of propane to propene is an important attempt towards developing an alternative or complement to existing propane dehydrogenation processes. A process based on oxidative dehydrogenation (OXD) has potential advantages such as low energy consumption and no catalyst regeneration requirement. In previous report, we have demonstrated that alumina-supported Cs-doped Cr–Mo oxide has potential as a catalyst for propane oxidative dehydrogenation (POD). It exhibited the best performance among the samples tested [1]. The important improvements in performances are higher selectivity to propene and lower CO than CO_2 on the Cs-doped sample compared to chromium oxide/γ-Al_2O_3. This was shown to be due to modifications in the redox properties of the promoted catalyst. It may also possess low electrophilic oxygen species thereby improving the selectivity to propene. Therefore, this shows that it is possible to reduce deep oxidation by appropriately changing the composition of the catalyst based on the understanding of the interaction between the hydrocarbons and catalyst surface adsorbed species.

The interaction between the propane, propyl species or propene and catalyst surface can be further understood by studying the kinetics and mechanistic network of the reaction on the catalyst. Although several catalytic systems have been tested and reported for OXD, only a few of the reports consider the kinetic aspects of the reaction [2–9]. Supported transition metal oxides are usually used to activate the alkanes and dioxygen. The activation of the alkane is believed to be by the rate-determining abstraction of hydrogen atom to form alkyl species [10]. Further reactions that determine selectivities depend partly on the position of the hydrogen atom on the alkyl group (i.e. on primary, secondary or tertiary carbon) involved in the reaction. Depending on the catalyst employed, the reaction may be with lattice oxygen, thus following the Mars-van Krevelen mechanism [11,12]. Another study indicated that reaction of adsorbed alkane with the adsorbed oxygen occurred, thereby following the Langmuir–Hinshelwood (L–H) mechanism [13]. Reaction of adsorbed alkane with gas phase oxygen has also been reported [14]. In yet another

* Corresponding author. Tel.: +966 1467 6897; fax: +966 1467 8770.
E-mail address: baba@ksu.edu.sa (B.Y. Jibril).

1385-8947/$ – see front matter © 2004 Published by Elsevier B.V.
doi:10.1016/j.cej.2004.03.006

study, the mechanism was shown to involve desorbed propyl radicals with gas phase oxygen [6].

It is apparent that the kinetics and mechanisms depend on the catalytic system used in the studies. Generally, the catalytic oxidative dehydrogenation of propane and other lower alkanes over V-Mg-O catalysts produces mainly dehydrogenation and combustion products [3,6,11]. Similar behavior in POD was reported on rare-earth-oxide-containing catalysts. No oxygenates were observed, although there was a significant formation of ethene [6]. In the same report, olefins and oxygenates were formed with significant selectivity for the reaction on B_2O_3/Al_2O_3. Molybdenum-based systems in addition to alkenes produce acrolein [15]. These differences are believed to be associated with the nature of the kinetics and mechanism of the reaction on the catalysts and are not well understood [10].

For instance, Kung and coworkers [5] have shown that the reaction of alkyl species that leads to either dehydrogenation products or oxygenates follow different paths on V-based catalysts. On the other hand, Stern and Grasselli reported that after the rate determining step, a second homolytic primary C–H bond breaking leads to propene. The propene is the intermediate to acrolein in the POD on Ni-Co-Mo catalyst [16]. These reports appear to be contradictory [17]. However, whether the reactions leading to alkenes and/or oxygenates are in series or parallel depends on the nature of the catalysts and the hydrocarbon to oxygen ratio. Generally, oxidation reactions on transition metal oxides take place mainly by two different mechanisms—intrafacial and suprafacial [18]. The former involves reaction with lattice oxygen while the latter involves reaction with adsorbed oxygen on the catalysts. Controlling the suprafacial reaction is important in increasing the propene yield.

In this report, results of a brief study on the kinetics and mechanistic networks of the oxidative dehydrogenation of propane over Cs-doped $Cr–Mo/Al_2O_3$ are discussed. This may help towards further understanding of the catalytic process. Based on this understanding, the composition of the catalyst and/or the operating conditions of the reaction could be modified to improve the yield to the desired products.

2. Experimental

The catalysts were tested in a fixed-bed, quartz laboratory reactor, operated at atmospheric pressure, temperature ranges of 300–340 °C and feed flow rate of 75 cm^3/min—mixture of propane, oxygen and helium as a diluent. The reactor was a 70 mm long quartz tube of 7 mm internal diameter (i.d.) tapered to a 2-mm i.d. This removes the reaction gases from the reaction zone as fast as possible, thereby minimizing possible gas phase reactions. The temperature of the catalyst bed was monitored by a thermocouple placed on the reactor wall from outside. A temperature controller (Omega CN3000) was used to monitor the temperature. The actual temperature of the catalyst bed was calibrated in a separate experiment using a second thermocouple positioned in the center of the catalyst bed. This is the reaction temperature reported. The gases were of high purity, propane (99.99%), oxygen (99.99%), and helium (99.99%) obtained from Linde. They were supplied from cylinders at laboratory temperature, passed through microfilters for additional purification and delivered to the reactor preheat zone. Omega electronic mass flow controllers controlled the gases. One gram of the 20–40 mesh size granules of each of the catalysts was each placed in the reaction zone of the reactor and supported on quartz wool directly above the junction of this section with the bottom. In each case, the catalyst was pretreated in a stream of oxygen for 30–45 min, at 450 °C. The line was then evacuated with helium at the same temperature for 30 min. Thereafter; the reactant gases were metered through the reactor at desired compositions and temperatures.

A gas chromatograph (HP6890) was used for an online analysis of both the feed and products streams. The products flowed directly through a heat-traced line to the GC sampling valve. The hydrocarbons; CH_4, C_2H_6, C_2H_4, C_3H_8 C_3H_6, C_4H_{10} and C_4H_8 were separated by HP-PLOT column and analyzed with flame ionization detector (FID), while O_2, CO and CO_2 were separated by MS and HayeSep-R column and analyzed with thermal conductivity detector (TCD). All GC analyses were performed online by software—HP Chemstation—provided with the equipment.

The catalyst particles sizes range and reaction temperature were chosen to minimize mass transfer limitations, based on a separate preliminary experiment. Feed composition was varied to obtain the conversions and selectivities, but the residence time was maintained at 0.60 s. A blank test without a catalyst or with quartz granules in the reactor showed negligible conversion of propane at the reaction conditions. Three runs were performed for each experimental point. The average values are reported. The values were reproducible within ±6%. Thus, sets of kinetic data were collected with negligible deactivation and the catalyst was presumably at same condition. The products distributions were determined at low conversion (<8%) to maintain differential conditions in the reactor. Carbon balances were typically better than 95%. The performance of each catalyst is reported based on the following: conversion is defined as the mole fraction of feed carbon present in the reaction products, while selectivity is the fraction of product carbon in a particular product. Details on preparation of the catalyst—Cs-doped 10 wt.% Cr-Mo (4:1)/γ-Al_2O_3—and the experimental procedure are as described elsewhere [1,19].

3. Results and discussion

3.1. Reaction network

The major products are propene and CO_X. Fig. 1 shows the change in selectivities to C_3H_6 and CO with propane conversion at 300 °C. No CO_2 was observed at this temperature.

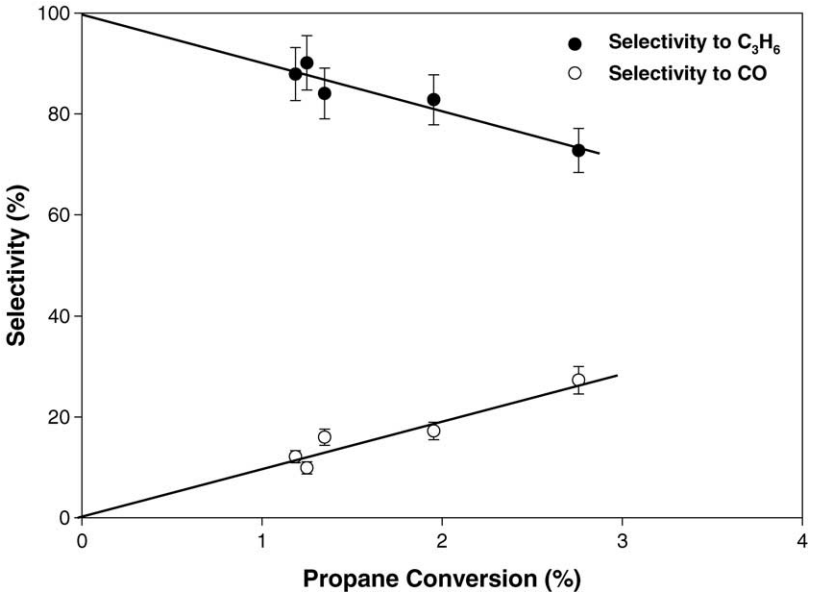

Fig. 1. Change in selectivity with propane conversion at 300 °C.

Extending a line through the selectivities to low conversion suggests that there is 100% selectivity to propene and 0% selectivity to CO at 0% conversion, thus indicating that propene is a primary product while CO is a secondary product. Propene is an exclusive primary product at the conditions used and CO is evidently produced by subsequent reaction of propene at higher conversions similar to earlier reports [18,20–22]. The distribution of propene and CO is maintained at higher temperature (320 °C) as shown in Fig. 2. Extending the selectivities to 0% conversion shows that CO is a secondary product. In addition, CO_2 is produced. The CO_2 appears to maintain a finite selectivity at 0% conversion, with corresponding decrease in propene selectivity to about 95%. This suggests that as the temperature increases, catalyst sites or oxygen species responsible for deep oxidation of propane to CO_2 are activated. It indicates that a high activity of lattice oxygen leads to overoxidation to CO_2. It further shows that there are different and unique oxygen species associated with separate sites for production of propene and CO_2. This is in addition to possible contributions from electrophilic attack on the propene by surface adsorbed oxygen at the higher temperatures. As shown in Fig. 3, increase in temperature to 340 °C maintains the trends observed at lower temperatures. The low temperature observation is similar to that reported

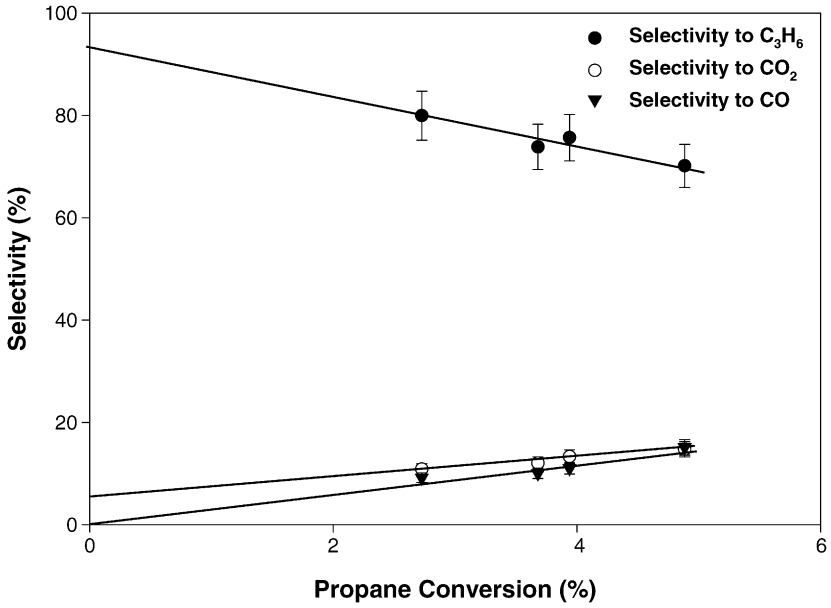

Fig. 2. Change in selectivity with propane conversion at 320 °C.

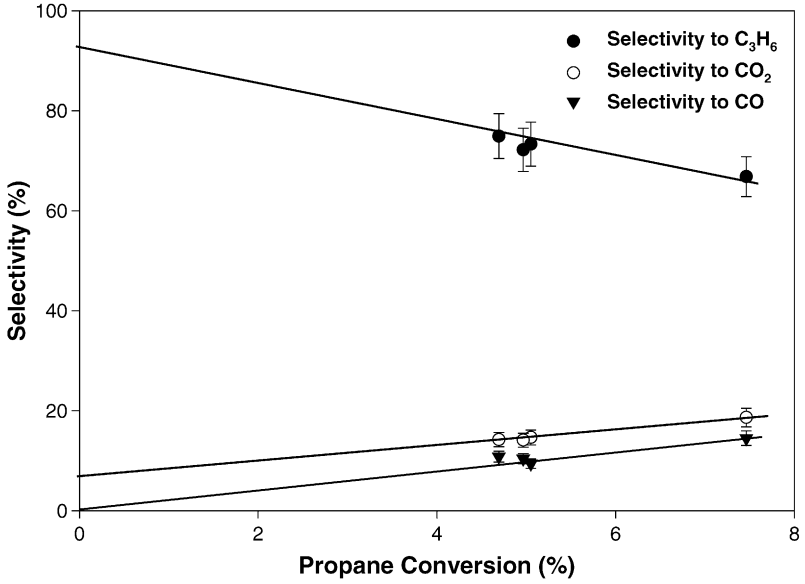

Fig. 3. Change in selectivity with propane conversion at 340 °C.

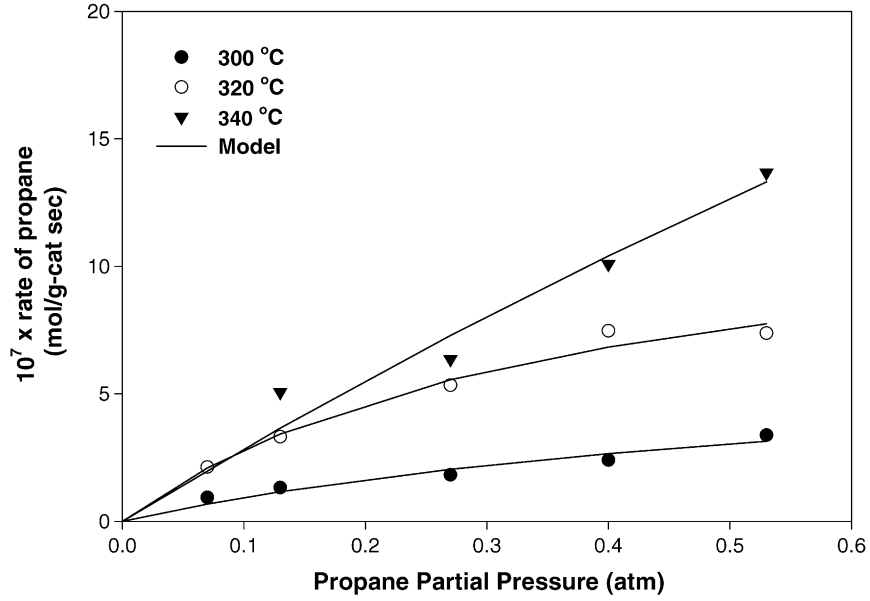

Fig. 4. Dependence of propane consumption rate on propane partial pressure (P_P) at oxygen partial pressure (P_O) of 0.13 atm.

on Ni–Co–molybdate where it was concluded that propene was the exclusive primary product while CO and CO_2 were solely produced by subsequent reaction of propene [16]. On the contrary, at high temperature CO_2 could also be produced as a primary product as shown by the results at 340 °C.

The results could be described by Scheme 1. After the rate-determining production of propyl species, further reaction of the propyl species determines the selectivity of the reaction [23,24]. (i) The propyl species may react instantaneously by β-elimination to produce propene, as indicated by step 2. (ii) It may react with neighboring electrophilic surface adsorbed oxygen and/or lattice oxygen to produce CO_X as major product (path: 3 → 4 → 5 → 6). This depends on the activity of the oxygen and reaction temperature. Highly active oxygen, perhaps at high temperatures, may lead to production of CO_X [25]. No C_2H_4 was observed at the conditions employed. (iii) The reaction in (ii) could take place between propyl species

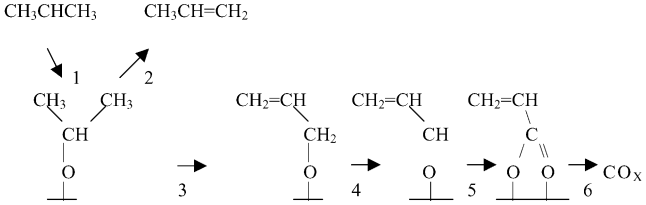

Scheme 1.

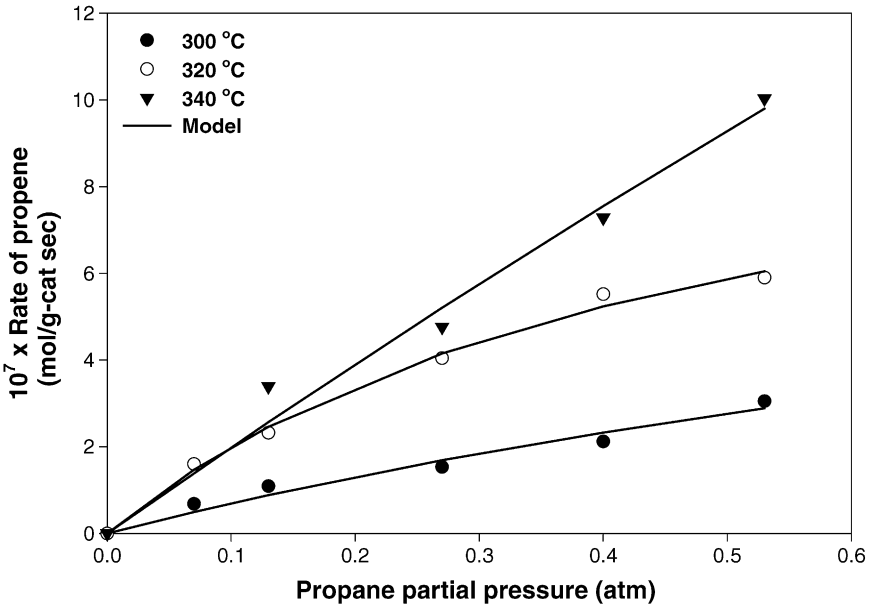

Fig. 5. Dependence of propene production rate on P_P at P_O of 0.13 atm.

and gas phase oxygen in the close vicinity of the catalyst surface and (iv) the propyl may move into the gas phase where further reactions take place [24]. Reactions (iii) and (iv) have been observed by Andersson [14] and Buyevskaya and Baerns [6], respectively.

The result tentatively shows that the reaction network involves propene as primary product and CO as a secondary product at low temperature, in agreement with earlier reports [18,20,21]. At higher temperature, the activity of lattice oxygen increases. This causes the further reaction of propyl species to CO_X thereby exhibiting CO_2 with a finite selectivity at low conversion, thus suggesting that it is a primary product [22].

3.2. Reaction kinetics

Figs. 4–7 show changes of rates of C_3H_8, C_3H_6, CO and CO_2 with propane partial pressure (P_P) at an oxygen partial pressure (P_O) of 0.13 atm and reaction temperatures of 300–340 °C. The points indicate the experimental values while solid lines show the calculated rates. Figs. 4 and 5 show variations in the rates of propane consumption and propene

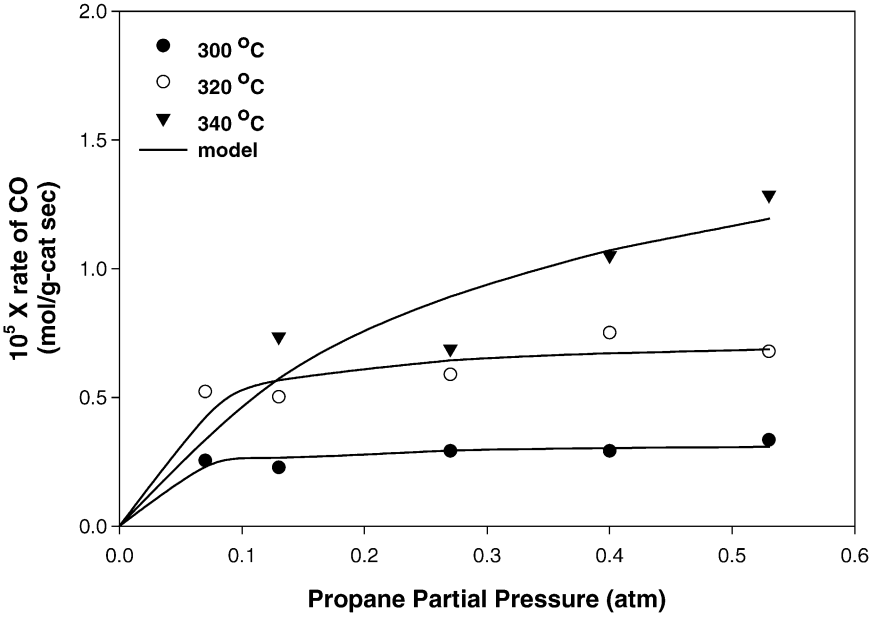

Fig. 6. Dependence of CO production rate on P_P at P_O of 0.13 atm.

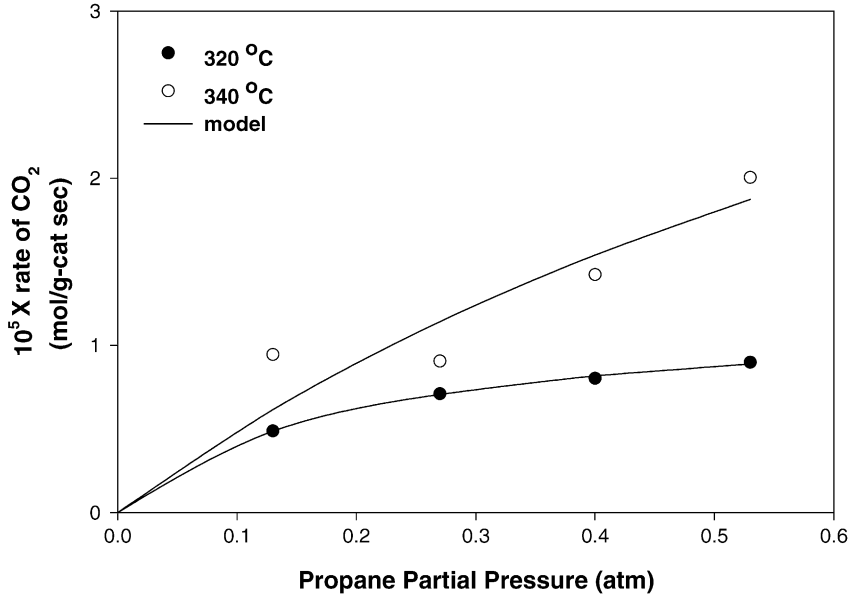

Fig. 7. Dependence of CO_2 production rate on P_P at P_O of 0.13 atm.

production with P_P, respectively. The figures show first-order behavior at low partial pressure of propane. At higher partial pressure, the relation becomes non-linear, thereby following a Langmuir-type rate expression. This shows a typical rate–partial pressure relation for the oxidative dehydrogenation reactions on redox catalysts where one of the adsorbed reactants is in equilibrium with the gas phase. On the redox catalyst, the lattice oxygen has been shown to participate in the reaction [18,20]. The rate depends mainly on P_P. This is assuming that the lattice oxygen is replenished at a rate higher than or equal to that of removal. The rates of CO and CO_2 production with P_P are illustrated in Figs. 6 and 7, respectively. The rates of both CO and CO_2 show a non-linear increase with P_P similar to Figs. 4 and 5.

Fig. 8 shows that change in the rate of propane conversion is zero-order with respect to oxygen partial pressure. This is expected for the oxidation of hydrocarbon on redox metal oxide catalyst, assuming no mass transfer limitations. The reaction takes place between the adsorbed propane and lattice oxygen, thereby reducing the catalyst. If the rate of re-oxidation of the catalyst is fast compared with the rate of removal of lattice oxygen, the rate of propane reaction would be independent of P_O. This can be observed in the figure, especially at low temperature and P_O values of

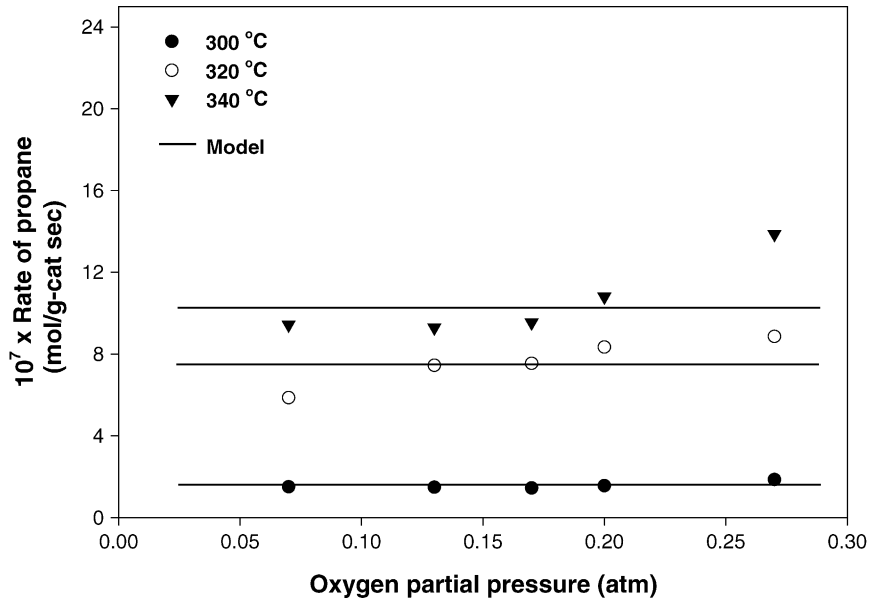

Fig. 8. Dependence of propane consumption rate on P_O at P_P of 0.27 atm (line indicates model equation).

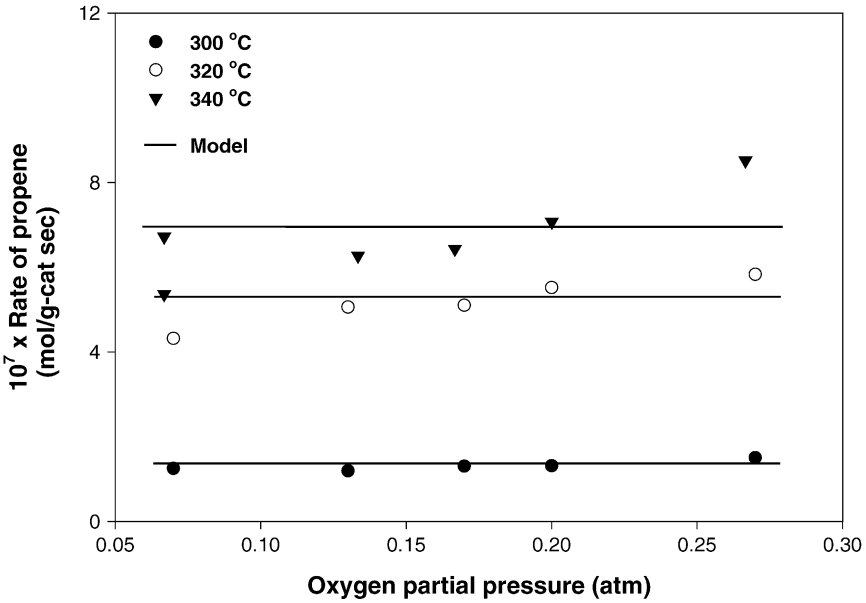

Fig. 9. Dependence of propene production rate on P_O at P_P of 0.27 atm (line indicates model equation).

0.06–0.2 atm. However, at higher temperatures, the rate appears to deviate from this trend, showing an increase with increase in oxygen partial pressure, especially at high values of P_O. Similar trend could be observed in the case of propene production rate as shown in Fig. 9. On the other hand, the rate of CO production shows stronger dependence on P_O as shown in Fig. 10. The rate increases with P_O. This indicates that surface adsorbed oxygen in equilibrium with gas phase oxygen is involved in the production of CO. Fig. 11 displays the rate of CO_2 formation which shows similar trends as CO with P_O. No CO_2 was produced at 300 °C.

The trend for the rates of propane conversion and propene formation suggest that at low temperature the rate is independent of oxygen partial pressure, thus following a Mars-Van Krevelen (MV) type mechanism while as the temperature increases the rate of lattice oxygen removal becomes significant perhaps higher than the rate of re-oxidation. The rate of lattice oxygen mobility has been reported to increase with temperature [26]. Thus, as the temperature increases, perhaps and especially at higher oxygen partial pressure, the availability of lattice oxygen increases. The abstracting of hydrogen from both propane and propyl species increases thereby making the rate to deviate from Mar-van Krevelen mechanism.

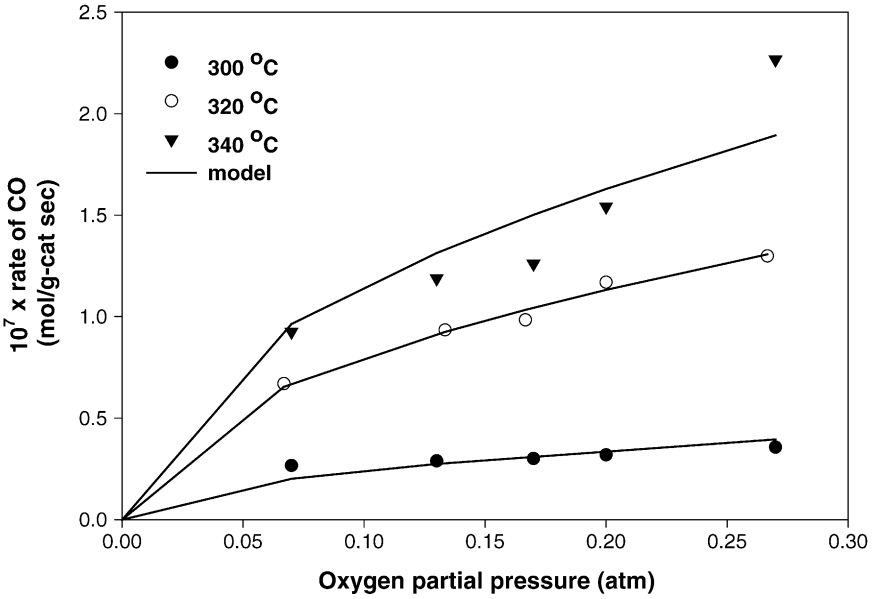

Fig. 10. Dependence of CO production rate on P_O at P_P of 0.27 atm.

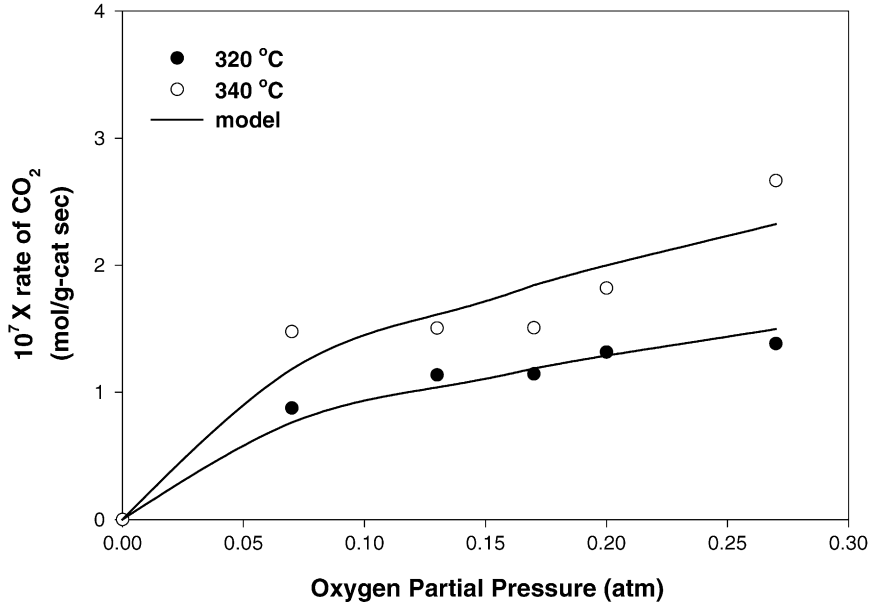

Fig. 11. Dependence of CO_2 production rate on P_O at P_P of 0.27 atm.

3.3. Kinetics model

The different trends shown by the rates of propane consumption and CO_X production indicate that the two reactions occur by different mechanisms. Perhaps the main difference is in the type of oxygen involved in the reaction. Oxidative dehydrogenation of propane is described by a Mars-van Krevelen mechanism. Langmuir–Hinshelwood (L–H) and Rideal–Eley mechanisms were also tested, but found to be less satisfactory. The deep oxidation to CO_X, on the other hand, is described by a L–H mechanism. The rates of CO and CO_2 formation could be fitted to a rate expression with half-order in oxygen partial pressure indicating dissociative adsorption of oxygen on the catalyst surface. The experimental observations are shown as points while the calculated rates are shown by solid lines in Figs. 4–11. There is good agreement between the calculated and observed rates. This suggests that the kinetic models are consistent with the experimental data within the condition studied. Values of model parameters are given in Table 1. The propane consumption rate is further analyzed using the MV rate expression given by Eq. (1) and its linear form in Eq. (2) [20]. The rate constants obtained are given in Table 2. Within the limit of calculation errors, the Arrhenius expression for the rate constant of propane consumption was used to evaluate the activation energy for the reaction giving a value of 18.8 kcal/mol. This is a typical value for propane oxidative dehydrogenation reactions [18,20].

Table 1
Kinetic model parameters[a] for rates of propane consumption and propene, CO_2 and CO production on Cs–CrMo–oxide/γ-Al_2O_3

	Temperature (°C)		
	300	320	340
$k'_{C_3H_8} \times 10^7$ (mol/g-cat s)	7.13	12.97	94.42
$k'_{C_3H_6} \times 10^7$ (mol/g-cat s)	4.95	8.75	65.13
$k'_{CO_2} \times 10^7$ (mol/g-cat s)	–	2.27	17.16
$k'_{CO} \times 10^7$ (mol/g-cat s)	7.52	6.82	20.58
$K_{C_3H_8}$ (Pa^{-1})	1.49	2.75	0.31

[a] Data in Figs. 4–7 are fitted to Langmuir-type rate expression, $r_i = (k'' P_{C_3H_8}/(1 + K_{C_3H_8} P_{C_3H_8}))$, while the data in Figs. 10 and 11 are fitted to $r_i = k P^{1/2}$. In the table, $k' = (k''/K)$.

Table 2
Rate constants for propane consumptions fitted to Eq. (2)

Propane oxidation (rate constant, mol/g-cat s Pa)	Reaction temperature (°C)		
	300	320	340
$k_1 \times 10^9$	1.69	3.56	4.93
$k_2 \times 10^9$	1.42	4.79	7.15

$$r_{C_3H_8} = \frac{2k_1k_2 P_{C_3H_8} P_{O_2}}{k_1 P_{C_3H_8} + 2k_2 P_{O_2}} \quad (1)$$

$$\frac{P_{O_2}}{r_{C_3H_8}} = \frac{1}{2k_2} + \frac{P_{O_2}}{k_1 P_{C_3H_8}} \quad (2)$$

where k_1 is the rate constant for propane consumption and k_2 is the rate constant for catalyst reoxidation.

4. Conclusion

The alumina supported Cs-doped Cr–Mo oxide has been found to be active in propane oxidative dehydrogenation. A study of the kinetics of the reaction on the catalyst at 1 atm and 300–340 °C shows that propane is oxidatively dehydrogenated to propene. CO appeared to be a secondary product produced from further oxidation of propene. CO_2 exhibited

a finite selectivity at low propane conversion, thus suggesting that it is mainly produced directly from propane. The rates of propane consumption, propene and CO_X production show Langmuir-type dependence on propane partial pressure. Propane consumption and propene production rates show no significant dependence on oxygen partial pressure. The CO_X rates were fitted to a half-order dependence relation in oxygen partial pressure indicating that the oxygen is dissociatively adsorbed on the catalyst surface. Although both propene and CO_2 are primary products, the difference in their dependence in oxygen indicates that different types of oxygen are involved in their reactions paths.

References

[1] B.Y. Jibril, S.M. Al-Zahrani, A.E. Abasaeed, R. Hughes, in: Proceedings of the 17th International Symposium on Chemical Reaction Engineering (ISCRE17), August 24–28, 2002, Hong Kong.
[2] C. Resini, M. Panizza, L. Arrighi, S. Sechi, G. Busca, R. Miglio, S. Rossini, Chem. Eng. J. 89 (2002) 75.
[3] S. Albonetti, G. Blanchard, P. Burattin, F. Cavani, S. Masetti, F. Trifiro, Catal Today 42 (1998) 283.
[4] J. Le Bars, J.C. Vedrine, A. Auroux, S. Trautmann, M. Baerns, Appl. Catal. A 88 (1992) 179.
[5] O.S. Owen, M.C. Kung, H.H. Kung, Catal. Lett. 12 (1992) 45.
[6] O.V. Buyevskaya, M. Baerns, Catal. Today 42 (1998) 315.
[7] N. Boisdron, A. Monnier, L. Jalowiecki–Duhamel, Y. Barbaux, J. Chem. Soc. Faraday Trans. 91 (1995) 2899.
[8] G. Busca, V. Lorenzelli, G. Oliveri, G. Ramis, Stud. Surf. Sci. Catal. 82 (1994) 253.
[9] P. Concepcion, A. Galli, J.M. Lopez Nieto, A. Dejoz, M.I. Vazquez, Topics Catal. 3 (1996) 451.
[10] H.H. Kung, M.C. Kung, Appl. Catal. A 157 (1997) 105.
[11] F. Cavani, F. Trifiro, Catal. Today 24 (1995) 307.
[12] D.L. Stern, R.K. Grasselli, J. Catal. 167 (1997) 560.
[13] M. Huff, L.D. Schmidt, J. Catal. 149 (1994) 127.
[14] S.L.T. Andersson, Appl. Catal. A 112 (1994) 209.
[15] D.L. Stern, R.K. Grasselli, J. Catal. 167 (1997) 550.
[16] D.L. Stern, R.K. Grasselli, J. Catal. 167 (1997) 570.
[17] M. Baldi, E. Finocchio, C. Pistarino, G. Busca, Appl. Catal. A 173 (1998) 61.
[18] J.N. Michaels, D.L. Stern, R.K. Grasselli, Catal. Lett. 42 (1996) 139.
[19] B.Y. Jibril, S.M. Al-Zahrani, A.E. Abasaeed, R. Hughes, Catal. Comm. 4 (2003) 579.
[20] E.A. Mamedov, S.N. Shaikh, Arabian J. Sci. Eng. 24 (1C) (1999) 27.
[21] K. Bahranowski, G. Bueno, B. Cortes Corberan, F. Kooli, E.M. Serwicka, R.X. Valenzuela, K. Wcislo, Appl. Catal. A: General 185 (1999) 65.
[22] M. Baldi, E. Finocchio, F. Milella, G. Busca, Appl. Catal. B 16 (1998) 43.
[23] K. Chen, A. Khodakov, J. Yang, A.T. Bell, E. Iglesia, J. Catal. 186 (1999) 325.
[24] F. Cavani, F. Trifiro, Catal. Today 51 (1999) 561.
[25] A. Pantazidis, S.A. Bucholz, H.W. Zanthoft, Y. Schuurman, C. Mirodatos, Catal. Today 40 (1998) 207.
[26] G.I. Golodets, Stud. Surf. Sci. Catal. 15 (1982) 1.